LTE Uplink Aggregate Interference Measurement System

Eric D. Nelson

Technical Memorandum

LTE Uplink Aggregate Interference Measurement System

Eric D. Nelson

U.S. DEPARTMENT OF COMMERCE

Evelyn Remaley, Associate Administrator, performing the delegated duties of the Assistant Secretary of Commerce for Communications and Information

February 2021

DISCLAIMER

Certain commercial equipment and materials are identified in this report to specify adequately the technical aspects of the reported results. In no case does such identification imply recommendation or endorsement by the National Telecommunications and Information Administration, nor does it imply that the material or equipment identified is the best available for this purpose.

CONTENTS

FIGURES

TABLES

ABBREVIATIONS/ACRONYMS

AWS	Advanced Wireless Services
CDF	cumulative distribution function
CSMAC	Commerce Spectrum Management Advisory Committee
DC	direct current
dBi	decibels relative to isotropic
DISA	Defense Information Systems Agency
DoD	Department of Defense
DSO	Defense Spectrum Organization
DUT	device under test
EIRP	effective isotropic radiated power
FFT	fast Fourier transform
eNodeB	Evolved Node B
G/T	gain over thermal (noise)
I/Q	in-phase and quadrature
ITS	Institute for Telecommunication Sciences
LNA	low noise amplifier
LTE	Long Term Evolution
MKS	meter, kilogram, and second
PDF	probability density function
PRB	physical resource block
PUCCH	physical uplink control channel
PUSCH	physical uplink shared channel
SC-FDMA	single carrier-frequency division multiple access
SNR	signal-to-noise ratio
SST&D	Spectrum Sharing Test and Demonstration Program
TTI	transmission time interval
UE	user equipment
VSA	vector signal analyzer
WG	working group

LTE UPLINK AGGREGATE INTERFERENCE MEASUREMENT SYSTEM

Eric D. Nelson[1]

This technical memorandum describes a method to design, characterize and optimize a system for performing field measurements of aggregate interference from LTE user equipment transmissions. It explains the computation of the system's antenna gain over effective system temperature (G/T) and anticipated signal-to-noise ratio levels using typical assumptions. It also covers the appropriate vector signal analyzer settings for performing I/Q captures of LTE signals and relevant post-processing techniques.

Keywords: uplink, LTE, UE, aggregate interference, I/Q, capture, G/T, noise temperature

1. BACKGROUND

In July 2012, the NTIA Commerce Spectrum Management Advisory Committee (CSMAC) convened working groups (WGs) with membership from federal agencies and commercial wireless operators to investigate the feasibility of sharing spectrum between commercial and federal systems. The WGs' final 2013 reports provided the technical basis for the Federal Communications Commission's (FCC) Advanced Wireless Services 3 (AWS-3) auction, in accordance with the Report and Order (R&O) dated 31 March 2014 [1]. The R&O established service, allocation, and technical rules for the AWS-3 bands: 1695-1710 MHz, 1755–1780 MHz, and 2155–2180 MHz. It also established requirements for commercial wireless broadband licensees to coordinate with the federal agencies when seeking to build out systems in the 1755-1780 MHz band.

The Commercial Spectrum Enhancement Act [(CSEA) Public Law 108-494], as amended by the Middle Class Tax Relief and Job Creation Act of 2012 [Public Law 112-96] and the Spectrum Pipeline Act of 2015 [Public Law 114-74], authorized federal agencies to recover costs associated with engineering studies to determine the feasibility of spectrum sharing arrangements through transfers from the Spectrum Relocation Fund (SRF) established by the CSEA.

The Department of Defense (DoD) received approval for a number of transition plans for the AWS-3 bands, including the Spectrum Sharing Test and Demonstration (SST&D) Program. The SST&D Program includes studies to reexamine the modeling and simulation techniques adopted in the CSMAC WGs and the subsequent DoD/Industry WG.

DoD uses an aggregate interference modeling tool to evaluate coordination requests from wireless carriers and determine the effect of LTE user equipment (UE) on both terrestrial and airborne DoD systems. The SST&D program convened WGs to evaluate potential refinements in

---

that model based on research in propagation phenomena, LTE characteristics and DoD receiver characteristics.

Working under an interagency agreement in support of DoD, in 2017 ITS initiated a program to measure, in carefully selected scenarios, aggregate LTE uplink signal levels to facilitate comparisons between measured and modeled results. Since AWS-3 deployments (with LTE uplink transmissions in the 1755–1780 MHz range) were not available, the AWS-1 band (with LTE uplink transmissions from 1710 to 1755 MHz) was used as a proxy.

2. INTRODUCTION

Development of the ITS aggregate LTE UE uplink emissions measurement system and assessment of its operational characteristics occurred over the course of several months and required the procurement and integration of a high gain antenna and front end preselector. Following successful field trials, the author derived the system's characteristics and determined that the analysis techniques provided valuable insights into the various design requirements and tradeoffs.

This technical memorandum details the method used to characterize and optimize the system for sensitivity and dynamic range. Calibration techniques that permit measured power to be referenced to a common reference plane consistent with that used in aggregate interference models are covered. Judicious choices of sampling rate for the measurement receiver and use of post-processing parameters derived from LTE uplink characteristics are detailed. These permit power measurements to be expressed in the inherent bandwidths associated with LTE UE uplink transmissions.

While all of the individual elements of the system and analyses are covered in the literature, the author believes that an inclusive treatment of the subject would be of general interest to designers of general purpose measurement systems for radiated emissions.

3. MEASUREMENT SYSTEM

Consider an idealized measurement scenario overlooking a terrain-free city from a prominent overlook where all UEs transmit the same power and all paths are free space. It is clear that nearby UEs will dominate over more distant ones in this situation. For example, since free space loss exhibits a 6 dB/octave characteristic, UEs twice as far away as nearby ones will be received at 6 dB less power. By extension, a configuration in which a receiver is placed 1 km from a city that is 8 km deep results in the furthest UEs contributing 18 dB less power than the nearest ones. By setting the receiver back from a city this effect can be reduced. For example, an 8 km setback from a 8 km deep city compresses the pathloss into a 6 dB range between the nearest and furthest UEs. This reduces the dynamic range requirements of the measurement system and, in particular, allows it to be configured for greater sensitivity without the risk of system overloads from strong nearby transmissions. This also provides more margin to accommodate UE transmissions that are attenuated by clutter, i.e. buildings or foliage.

Generally speaking, an elevated location that is line of sight to a substantial population center is desired. Since the LTE scheduler adjusts UE transmitter power to achieve a target power at the eNodeB receiver, a receive antenna with a gain comparable to or greater than a typical eNodeB antenna is required. We also need a system with very good sensitivity since we will be trying to measure UEs that are farther away than a typical cell site radius.

We considered two instruments, a spectrum analyzer and a VSA. We found that a general purpose swept frequency spectrum analyzer is unable to simultaneously observe transmissions in the uplink band, since the occupied bandwidth ranges from 4.5 to 18 MHz. VSAs don't have this limitation. However, since VSAs have noise figures on the order of 10 dB, which degrades the total system noise figure, a low noise amplifier (LNA) with accompanying bandpass filter to reject strong out-of-band signals is necessary.

The minimal components for the system, then, are a) a high gain antenna (> 20 dBi) with large enough horizontal beamwidth to capture transmissions from a cross section of the population center, b) a short jumper cable to a preselector, i.e. a shielded RF enclosure containing a bandpass filter followed by an LNA, c) a coaxial cable from the preselector mounted adjacent to the antenna on an elevated mast to a bulkhead connector on the mobile measurement vehicle, d) a final coaxial cable which terminates at e) the measurement instrument as shown in Figure 1.

We will derive the signal-to-noise ratio (SNR) for this system based on its figure of merit, G/T, or antenna gain over thermal noise, based on typically available antennas, and assess the measurement system's suitability and optimality for sensitivity and dynamic range. Finally, as a design check, we will derive available noise power at the input to the measurement receiver from the system effective noise temperature and compare it to measured results.

3.1 System Block Diagram and Received Power Calculation

The measurement system is illustrated in Figure 1, in which typical reference planes of interest (at the antenna terminal, LNA input and receiver input) are indicated.
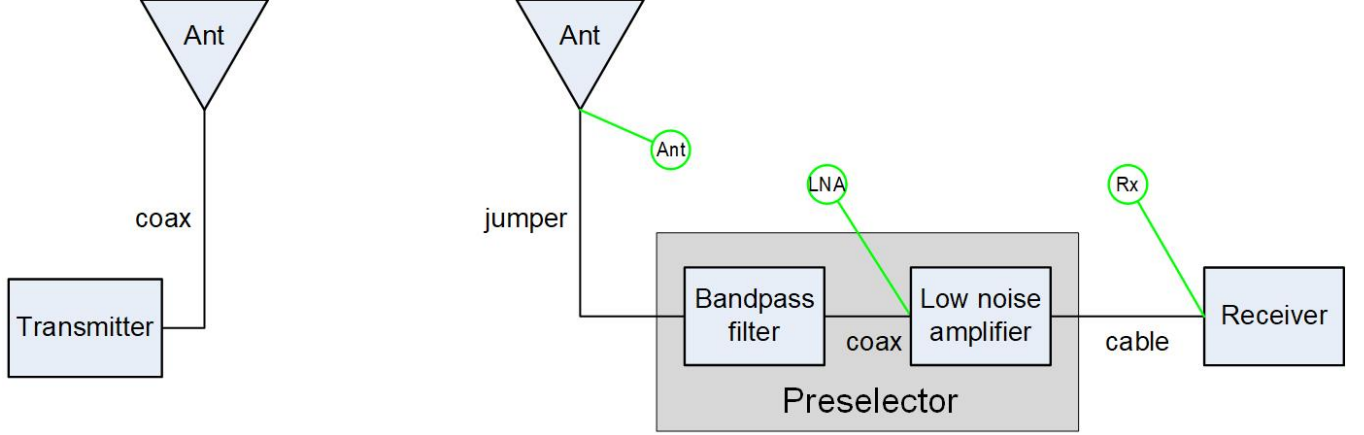
Figure 1. Receive system block diagram

Without loss in generality, we may neglect losses and impedance mismatches from the coax in the transmit system, and write the Friis transmission equation for the received power at the receive antenna terminal:

$$p_{Ant} = p_{Tx} g_{Tx} g_{Rx} \left(\frac{c}{4\pi df} \right)^2 \tag{1}$$

where p_{Tx} is the power input to the transmit antenna and p_{Ant} is the power at the receive antenna terminal in watts, g_{Tx} and g_{Rx} are the transmit and receive antenna gains in linear units ($0 \leq g \leq 1$), d is the distance between the transmitting and receiving antennas in meters, c is the speed of light in m/s, and f is the frequency in Hertz. Unless otherwise specified, lower case variables indicate linear terms while upper case variables represent their corresponding decibel values. All other terms are in meter, kilogram, and second (MKS) units.

We are interested in the available power at the input of the LNA, since by convention this is the customary reference plane used in system noise figure or antenna temperature computations. Because all of the elements between the antenna terminal and the input of the LNA are passive, we can combine them into a single (positive) feed loss, L_{feed}, where

$$L_{feed} = L_{jumper} + L_{filter} + L_{coax} \ \text{(dB)} \tag{2}$$

which can also be expressed as a dimensionless gain ($0 \leq g_{feed} \leq 1$) given

$$l_{feed} = 10^{\,L_{feed}/10} \text{and } g_{feed} = 1/l_{feed} \tag{3}$$

Inclusion of the feed gain (or loss) term transfers the reference plane from antenna terminal to the input of the LNA:

$$p_{LNA} = p_{Tx} g_{Tx} g_{Rx} g_{feed} \left(\frac{c}{4\pi df} \right)^2 = \frac{p_{Tx} g_{Tx} g_{Rx}}{l_{feed}} \left(\frac{c}{4\pi df} \right)^2 \tag{4}$$

5

Expressing this equation in decibels, where, in general, $P = 10 \log(p)$ and $G = 10\log(g)$, yields:

$$P_{LNA} = P_{Tx} + G_{Tx} + G_{Rx} - L_{feed} - 20 \log(d)$$
$$- 20 \log(f) + 20 \log\left(\frac{c}{4\pi}\right) \text{ (dBW)} \tag{5}$$

The last three terms represent the (positive) free space path loss in dB:

$$L_{path} = 20 \log(d) + 20 \log(f) - 20 \log\left(\frac{c}{4\pi}\right) \text{ (dB)} \tag{6}$$

while the first two terms represent the effective isotropic radiated power (EIRP):

$$P_{Tx} + G_{Tx} = EIRP \text{ (dBW)} \tag{7}$$

such that the equation reduces to this simple form:

$$P_{LNA} = EIRP - L_{path} + \left(G_{Rx} - L_{feed}\right) \text{ (dBW)} \tag{8}$$

3.2 System Noise Power and Signal-to-Noise Ratio

The received SNR, which is characteristically measured at the input to the LNA, is by definition:

$$snr_{LNA} = \frac{p_{LNA}}{n_{LNA}} \text{ or } SNR_{LNA} = P_{LNA} - N_{LNA} \text{ (dB)} \tag{9}$$

For a typical terrestrial antenna with a 0° elevation angle, the antenna beam will only subtend a half space of earth, so we expect the antenna temperature to be less than the standard temperature customarily used in system noise temperature computations (290 K or 62 °F), as we are combining roughly equal parts of noise from the earth ($\sim$ 300 K) with that from the atmosphere ($\sim$ 70 K) [3]. This has the effect of decreasing the measured noise from that which is measured if the feed is terminated with a 50 Ω load, which by convention is assumed to be 290 K. To account for this effect, we will derive the available power using noise temperature techniques.

First, we derive the total effective noise temperature at the antenna terminal and then transfer the reference plane to the LNA input. The noise temperature at the antenna terminal is due to the antenna temperature itself plus the total effective system noise referenced to the antenna terminal:

$$T_{Tot|Ant} = T_{Ant} + T_{sys|Ant} \tag{10}$$

where $T_{Tot|Ant}$ is the total noise temperature referenced to the receiving antenna, T_{Ant} is the noise temperature of the receiving antenna, and $T_{sys|Ant}$ is noise temperature of the system referenced to the receiving antenna terminal, so that according to the Friis equation [3]

6

$$T_{sys|Ant} = T_{feed} + \frac{T_{LNA}}{g_{feed}} + \frac{T_{cable}}{g_{feed}g_{LNA}} + \frac{T_{Rx}}{g_{feed}g_{LNA}g_{cable}} \tag{11}$$

thus

$$T_{Tot|Ant} = T_{Ant} + T_{feed} + \frac{T_{LNA}}{g_{feed}} + \frac{T_{cable}}{g_{feed}g_{LNA}} + \frac{T_{Rx}}{g_{feed}g_{LNA}g_{cable}} \tag{12}$$

Assuming all components are at the standard temperature, T_0, of 290 K, a component's noise temperature may be determined from its noise factor, f, in linear units using:

$$T = T_0(f - 1). \tag{13}$$

Component specifications are typically given in noise figure F (in dB), which describes the additional noise contributed by the device. The (dimensionless) noise factor may be determined using:

$$f = 10^{F/10} \tag{14}$$

For passive components at the standard temperature, T_0, the noise figure in dB equals the (positive) loss in dB, i.e. F = L, so the noise factor, f, equals the dimensionless loss, l. Likewise, losses (in dB) may be converted to (dimensionless) gain using $g = 10^{-L/10}$.

For active components the (dimensionless) gain and noise factor are: $g = 10^{G/10}$ and $f = 10^{F/10}$, where G and F are the gain and noise figure in dB, respectively.

It can be shown [4] that the reference plane for the total effective noise temperature can be translated from the input to the output (and vice versa) of passive elements by the simple relations:

$$T_{sys,output} = gT_{sys,input} \text{ or } T_{sys,input} = \frac{T_{sys,output}}{g} \tag{15}$$

where g is the linear gain of the element ($0 \leq g \leq 1$). Therefore, taking into account the gain of the feed section, the total effective noise temperature referenced to the LNA input is

$$T_{Tot|LNA} = g_{feed}T_{Tot|Ant} \tag{16}$$

so

$$T_{Tot|LNA} = g_{feed}T_{Ant} + g_{feed}T_{feed} + T_{LNA} + \frac{T_{cable}}{g_{LNA}} + \frac{T_{Rx}}{g_{LNA}g_{cable}} \tag{17}$$

The noise power (in watts) available at the LNA input is simply

$$n_{LNA} = kT_{Tot|LNA}B \text{ (W)} \tag{18}$$

where k is Boltzmann's constant ($1.38064852 \times 10^{-23}\ \frac{\text{kg m}^2}{\text{s}^2\ \text{K}}$) and B is the equivalent noise bandwidth (Hz). Expressed in dBW, the noise at the LNA input is

$$N_{LNA} = 10\log(T_{Tot|LNA}) + 10\log(kB) \text{ (W)}. \tag{19}$$

Therefore, the signal to noise ratio at the LNA input is

$$SNR = P_{LNA} - N_{LNA} \tag{20}$$

or more completely:

$$SNR = EIRP - L_{path} + (G_{Rx} - L_{feed}) - 10\log(T_{Tot|LNA}) - \\ 10\log(kB). \tag{21}$$

Expressing the total effective noise temperature in dB and annotating the subscript with ",dB" to distinguish this from a linear representation of noise temperature,

$$T_{Tot|LNA,dB} = 10\log(T_{Tot|LNA}) \tag{22}$$

and substituting and rearranging terms yields:

$$SNR_{LNA} = EIRP - L_{path} + (G_{Rx} - L_{feed}) - T_{Tot|LNA,dB} - 10\log(kB) \tag{23}$$

It is common practice to combine the antenna gain with the feed loss and the total effective system temperature to yield the system figure of merit, G/T:

$$\frac{G}{T} = (G_{Rx} - L_{feed}) - T_{Tot|LNA,dB} \quad \left(\frac{\text{dB}}{\text{K}}\right) \tag{24}$$

thus

$$SNR_{LNA} = EIRP - L_{path} + \frac{G}{T} - 10\log(kB) \tag{25}$$

Note that for a scenario involving a fixed transmitter EIRP, pathloss, and receiver bandwidth any improvements in the system SNR are restricted to tradeoffs between receive antenna gain, feed losses and system noise temperature, which is largely dependent on the noise figure and gain of the LNA.

Consider a simple example in which we wish to detect an LTE user equipment (UE) transmission of 0 dBm (-30 dBW) at f = 1745 MHz in a single physical resource block (PRB), i.e. 180 kHz, using an antenna with 30 dBi of gain. Assuming each of the PRB's twelve 15 kHz subcarriers is of equal power we will use an equivalent noise bandwidth of 15 kHz in our computations, i.e. the power spectral density is -30 dBW + 10log(1/12) = -43.22 dBW in a

15 kHz bandwidth. Typical values for components used in the ITS measurement system are shown in Table 1.

First, the noise temperature contribution of each component is computed, T (K), then that noise is transferred to the LNA input reference plane, T_{LNA} (K). Finally, the noise temperatures are summed.

Table 1. Total Effective Noise Temperature Computation

Component	Gain	g	f	F (dB)	T (K)	TLNA (K)
Antenna	30				150	119.15
Feed	-1.0	0.79	1.26	1.00	75.1	59.64
LNA	37.0	5011.87	1.19	0.75	54.67	54.67
Cable	-3.0	0.50	2.00	3.00	288.6	0.06
Receiver			10.00	10.00	2610.0	1.04
Total						234.56

The gain over thermal for this system is thus

$$G/_T = (30 - 1) - 10\log(234.56) = 5.30 \text{ dB/K.} \tag{26}$$

Computing the SNR using this value, observe (in Figure 2) that under the idealized assumption of free space path loss we anticipate more than 34 dB of margin out to 10 km which will allow us to detect UEs that are line of sight or subject to modest amounts of clutter losses from buildings and foliage.
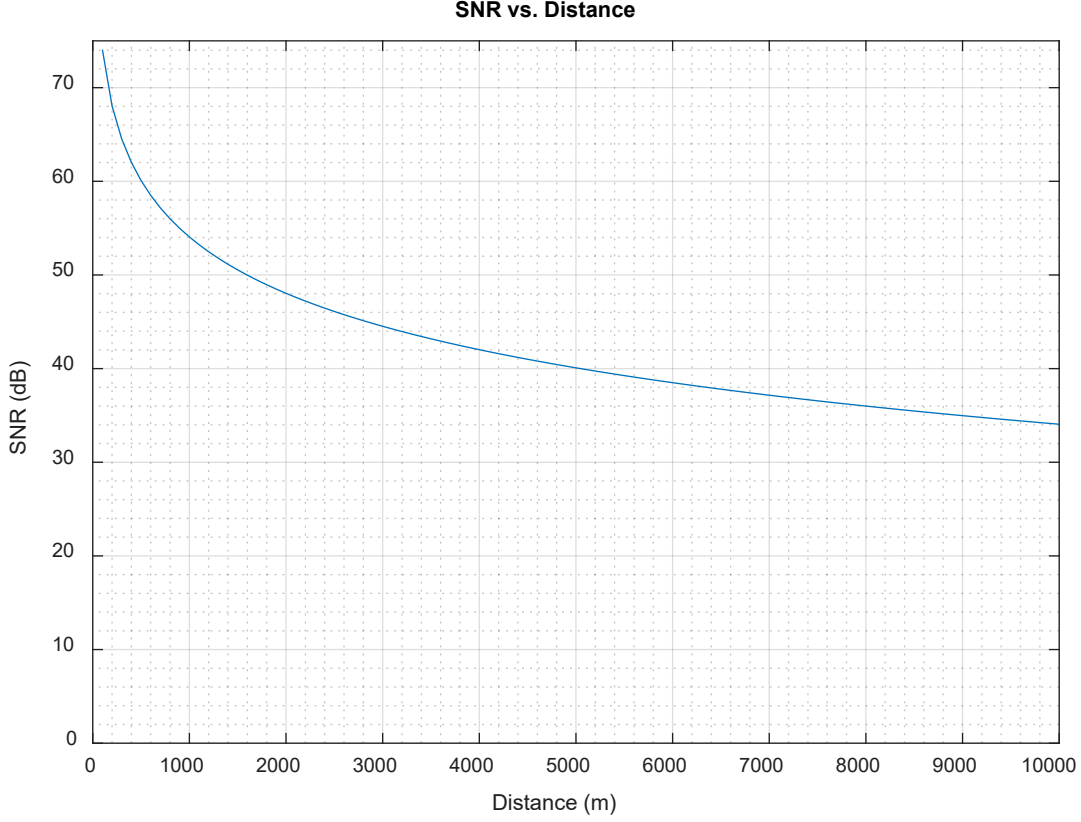
Figure 2. *SNR* vs. distance for a simplified scenario where f = 1745 MHz, B = 15 kHz, and *EIRP* = -30 dBW in a 180 kHz bandwidth

We have modeled all of the components as noiseless elements by referencing their noise contributions to the input of the LNA. By doing this, the total effective system noise can be transferred to other reference planes by adjusting for the gain of intervening stages. Therefore, the noise at the input of the receiver is

$$n_{Rx} = g_{LNA} g_{cable} n_{LNA} = g_{LNA} g_{cable} k T_{Tot|LNA} B \tag{27}$$

Using the numbers in Table 1, we can calculate the measured available noise power at the receiver

$$N_{Rx} = 10 \log(5011.87 \times 0.5 \times 234.56 \times 1.38x10^{-23} \times 15x10^3) \tag{28}$$
$$= -129.1 \text{ dBW}$$

while the noise floor for the receiver alone, which has a 10 dB noise figure, is:

$$N_0 = 10 \log(kT_0 B) + F_{Rx} = 10 \log(290 \times 1.38x10^{-23} \times 15x10^3) + 10 \tag{29}$$
$$= -152.2 \text{ dBW}$$

10

so the introduction of the high gain low noise amplifier has increased the measured noise floor at the receiver by approximately 23 dB.

Next, it is important to examine the tradeoffs between LNA gain and noise figure to achieve an optimal design (see Figure 3). Notice that beyond a certain point—approximately 25 dB—additional LNA gain offers negligible improvements in system G/T at the expense of reducing the dynamic range of the measurement system. Beyond this point G/T improvement is mostly dependent on selecting an LNA with a lower noise figure, increasing the antenna gain, or reducing the feed loss. As an aside, this plot demonstrates that the 37 dB gain LNA used in the ITS measurement system, which was simply drawn from existing stock, has suboptimal, excessive gain.
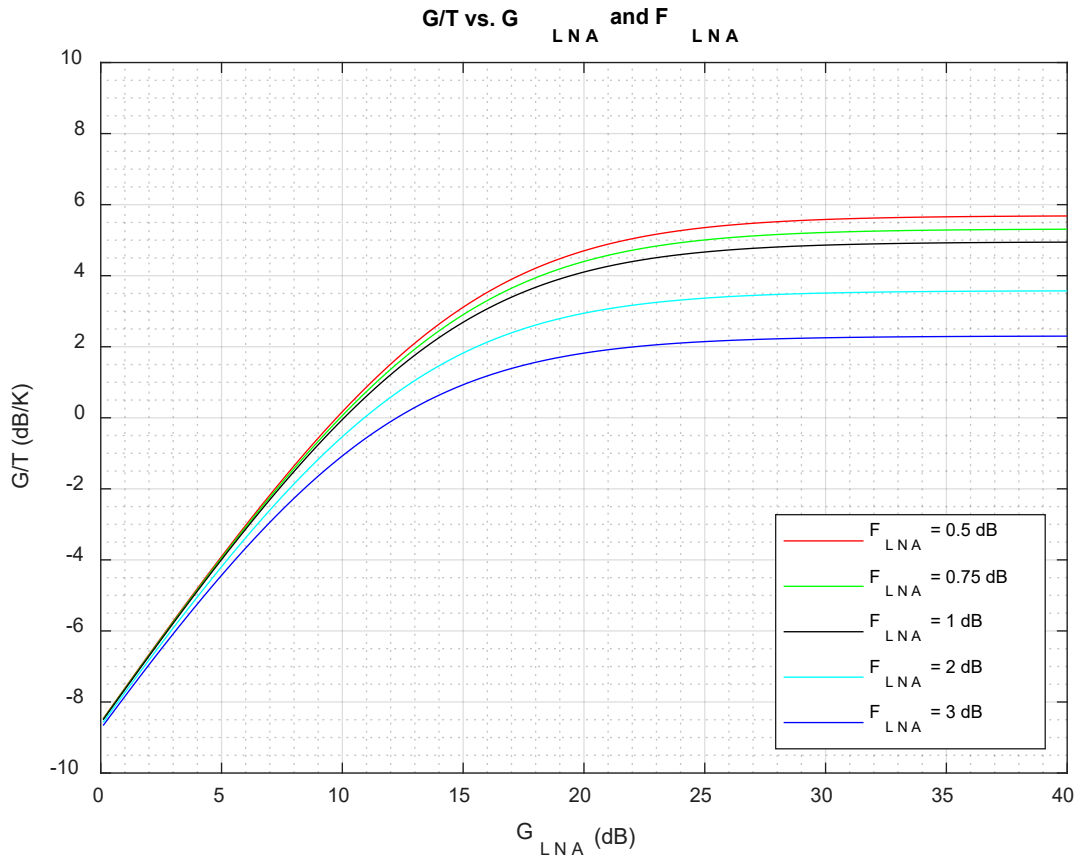
Figure 3. G/T assuming a fixed antenna gain but varying LNA gain and noise figure.

The above conclusion is based on a receiver with a noise figure of 10 dB. To gain a more general understanding of the amount of LNA gain necessary to overcome contributions from the receiver's internal noise, a contour plot relating G/T to the receiver noise figure and LNA gain under the following assumptions is shown in Figure 4.

$$G_{Ant} = 30 \text{ dBi}, L_{feed} = 1 \text{ dB}, F_{LNA} = 0.75 \text{ dB}, L_{cable} = 3 \text{ dB} \tag{30}$$
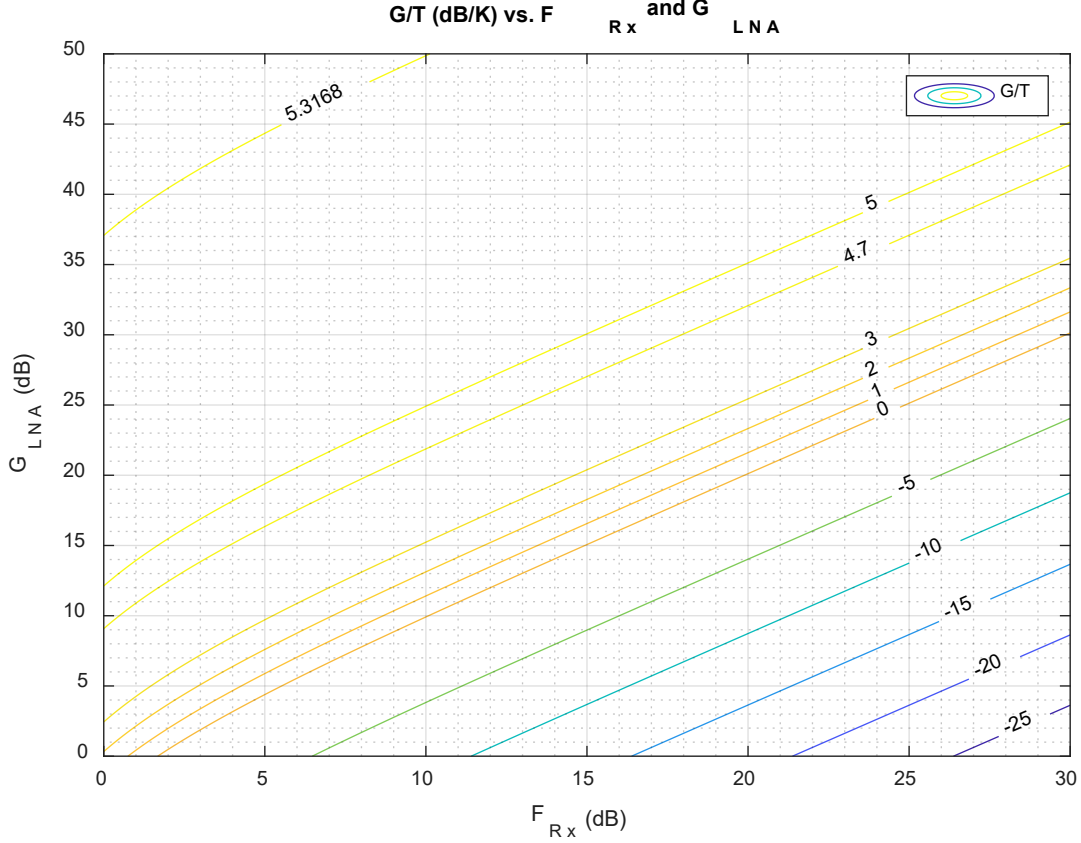
Figure 4. G/T contour plot for various receiver noise figures and LNA gains.

The maximum G/T for this configuration is shown at the upper left, i.e. 5.3168 dB/K. Consistent with earlier findings that higher LNA gains yield diminishing returns, observe in Figure 4 that only 0.32 dB improvement in G/T is achieved by increasing the LNA gain from 25 to 50 dB (for a receiver noise figure of 10 dB). Setting G/T = 5 dB/K as our performance target, observe that $G_{LNA} \approx F_{Rx} + 15$. This rule of thumb applies for systems with LNAs having typical noise figures (less than 2 dB) and for modest cable losses (less than 3 dB).

Using the following assumptions as the basis for further analysis:

$$G_{Ant} = 30 \text{ dBi}, L_{feed} = 1 \text{ dB}, F_{LNA} = 0.75 \text{ dB}, G_{LNA} = 25 \text{ dB} \tag{31}$$

we can assess the combined contribution to the total effective system noise temperature from the cable and the receiver recognizing that

$$T_{cable+Rx} = T_0(f_{cable}f_{Rx} - 1) = T_0(l_{cable}f_{Rx} - 1) \tag{32}$$

such that

$$T_{Tot|LNA} = g_{feed}T_{Ant} + g_{feed}T_{feed} + T_{LNA} + \frac{T_{cable+Rx}}{g_{LNA}} \tag{33}$$

Observe that G/T is constant where the product of the (linear) cable loss and the receiver noise factor is fixed as is illustrated in Figure 5. Consequently, to maintain a constant system noise temperature, a one-for-one improvement in receiver noise figure is required to offset increased cable losses (in dB). Alternatively, for a fixed receiver noise figure (such as 9 dB), we encounter only 0.3 dB of G/T degradation when cable losses are increased from 0 to 6.5 dB.
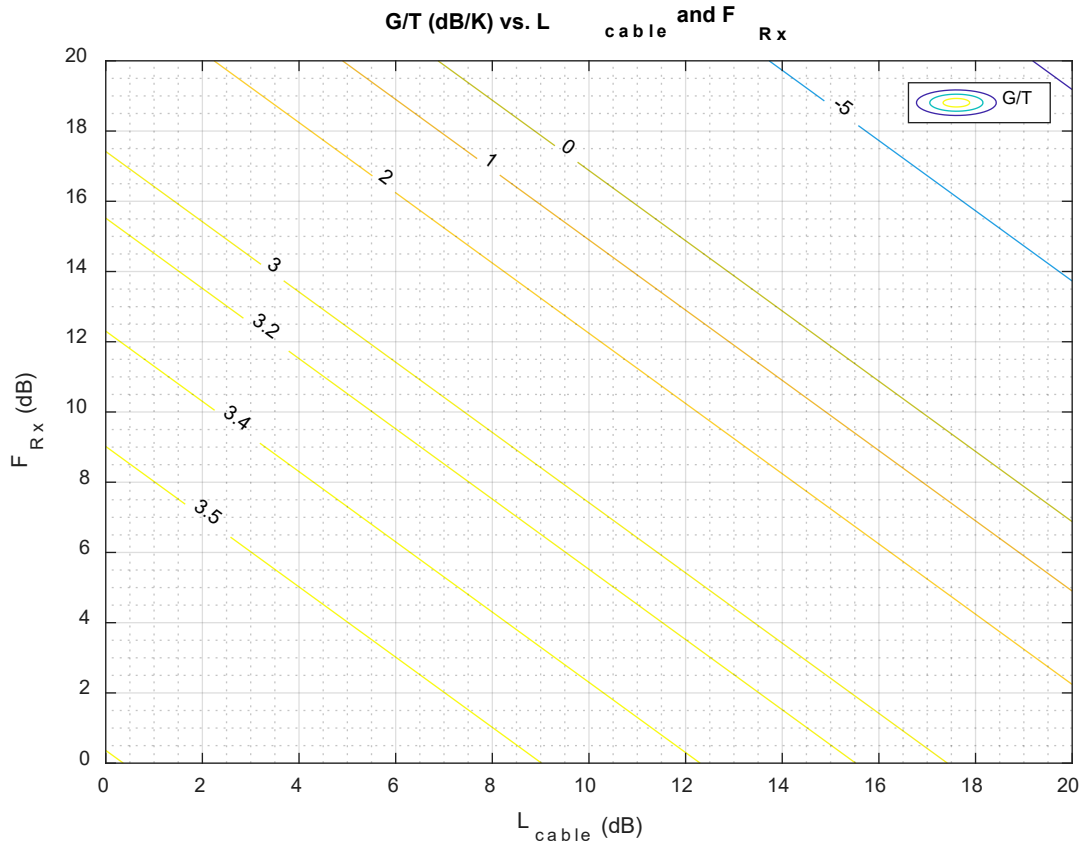
Figure 5. G/T contour plot for various receiver noise figures and cable losses.

3.3 LTE Uplink Characteristics

LTE UE transmissions occupy one or more contiguous 180 kHz PRBs that may change frequency, modulation and power every transmission time interval (TTI) of 1 ms. Each PRB in turn contains 12 subcarriers. A traditional swept frequency spectrum analyzer is unable to measure the time, frequency, and power variations in LTE uplink signals, since sweep times on the order of one TTI of 1 ms would be required to detect simultaneous transmissions over occupied bandwidths ranging from 4.5 to 18 MHz. Such rapid sweep times are not possible given the narrow resolution bandwidths needed to resolve 15 kHz LTE subcarriers. Instead, a VSA is the preferred means of capturing and post-processing aggregate UE emissions. VSAs are capable of capturing baseband in-phase and quadrature (I/Q) waveforms at a sample rate consistent with the UE's single carrier frequency division multiple access (SC-FDMA) transmission rate, permitting a faithful analysis or reproduction of the received signal.

To ensure the measurement system meets requirements, it is advantageous to determine its anticipated SNR performance under general assumptions for the transmitters' power spectral density and separation distance from the receive antenna. For example, what SNR do we expect to measure for an LTE uplink transmission in a single PRB (180 kHz) from a distance of 1 km at a power of 0 dBm at 1710 MHz, the lower end of the AWS-1 band?

The measurement receiver ITS used for uplink aggregate LTE UE measurements is a Keysight N9030B PXA spectrum analyzer which supports an optional VSA mode. At its greatest sensitivity the instrument has a noise figure of approximately 10 dB. To achieve maximum sensitivity and dynamic range a front end LNA is required. LNAs are typically broadband devices with pass bands in excess of the measurement range of interest. LNAs amplify signals outside the band of interest and are subject to frontend overload due to strong nearby transmitters such as commercial mobile downlink transmissions. Therefore, it is usually recommended to precede the LNA with a low insertion loss band pass filter. With such a design it is possible to achieve a system noise figure on the order of 3 dB, a 7 dB improvement in dynamic range which provides greater sensitivity to signals farther from the receiving system.

The PXA uses Model 89600 VSA software to capture baseband I/Q. There are a limited number of user accessible VSA settings [5] required to capture an LTE uplink transmission, as detailed in Table 2.

Table 2. Keysight PXA Baseband I/Q Capture Settings

Setting Name	Description	Typical Value
Center	The center frequency of the VSA capture	Set to the boundary between the center two subcarriers in the band of interest
Range	The upper bound for received channel power including frequencies outside the specified span	-42 dBm, which is the minimum input range
Span	The range of frequencies which are unimpaired by the instrument's built-in anti-aliasing filter	The span determines the sample rate, i.e. Rate = Span × 1.28
Record Length	The duration of the recording specified in seconds or number of samples	1-10 seconds

The primary consideration for optimal capture and post-processing of VSA data collections of LTE uplink signals is to ensure that the instrument's center frequency is positioned between two subcarriers in the uplink band—preferably the two center subcarriers. An example for a 10 MHz band is shown in Figure 6. This arrangement aligns the FFT bin center frequencies with the center of each subcarrier, and makes bin identification simpler. For example, the center frequency is between bins 512 and 513 in a 1024 point FFT. It also eliminates the direct current component in the FFT.
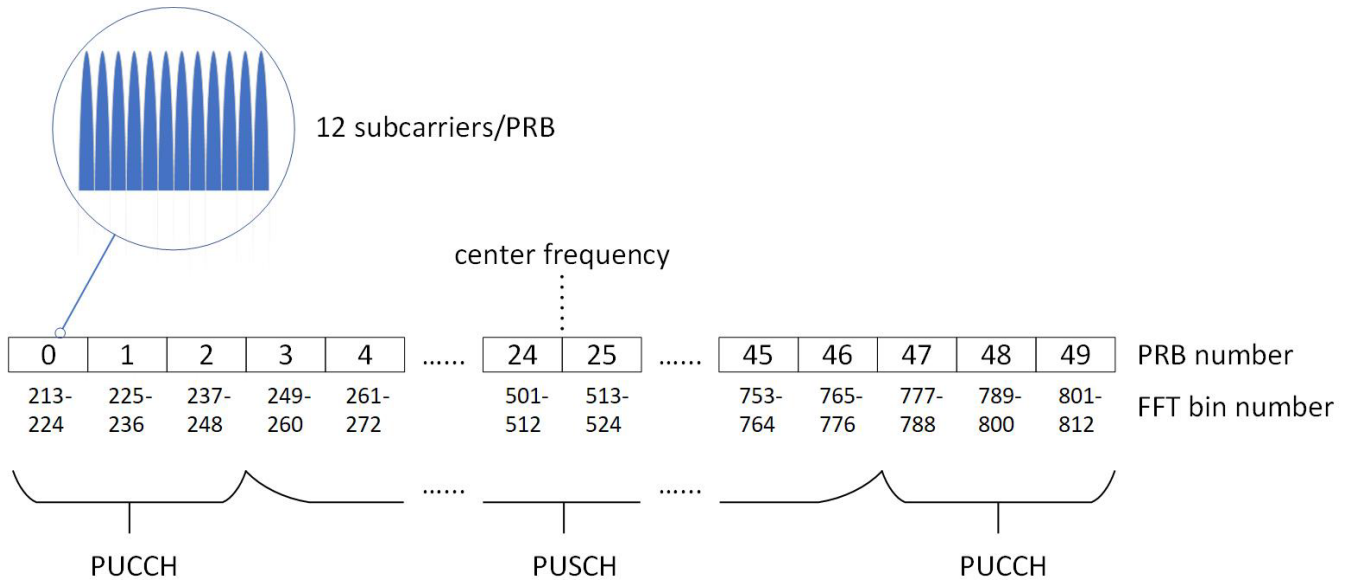
Figure 6. PRB and FFT bin identification for 10 MHz band.

Key LTE uplink physical layer parameters [6] are as follows.

Table 3. LTE Uplink Physical Layer Parameters

Channel Bandwidth (MHz)	5.0	10.0	15.0	20.0
Occupied Bandwidth (MHz)	4.5	9.0	12.0	18.0
Number of PRBs	25	50	75	100
Sampling Frequency (MHz)	7.68	15.36	23.04	30.72
FFT size	512	1024	1536	2048
Sub-carrier spacing (kHz)	15			
VSA Span (MHz)	6	12	18	24

3.4 I/Q Capture Post-processing

VSA captures are saved as MATLAB™ workspace files containing the following variables required for post-processing:

Table 4. Keysight PXA Baseband I/Q Capture Metadata

Name	Description	Typical Value
FreqValidMax	The upper boundary of the span in Hz	
FreqValidMin	The lower boundary of the span in Hz	
InputCenter	The center frequency of the capture in Hz	
InputRange	The maximum allowable voltage	0.0025 V = -42 dBm
InputRefImped	Reference impedance in Ohm	50
TimeString	Datetime of the beginning of the capture according to the VSA's internal clock	
XDelta	Interval in seconds between samples	$1/(1.28(FreqValidMax - FreqValidMin))$
XUnit	Units for time dimension of the capture in seconds	Sec, i.e. seconds
Y	I/Q sample values	
YUnit	I/Q sample units	Volts

4. DATA POST-PROCESSING

4.1 General Purpose Power Calculations

Baseband I/Q captures are collected using a variety of situation-dependent PXA span and center frequency settings based on the AWS-1 LTE carriers and out of band emissions of interest. In all instances, the PXA's span and center frequency should be configured to produce 15 kHz FFT bins aligned with the uplink subcarrier frequencies.

MATLAB post-processing scripts employing Welch's method [7] with zero overlap are used to develop periodograms and other analysis artifacts. In other words, an I/Q capture of length L is split into M segments of length N. Each N-point time domain segment is windowed and the FFT computed. The resultant N × M array contains power in 15 kHz bins for L/N time increments which are each 1/15 ms in duration. The core of the MATLAB script follows.

```
fs=1/XDelta;        % sampling frequency in Hz
binbw=15000;        % FFT bin size in Hz
nbins=fs/binbw;     % the number of bins in the FFT

w=hann(nbins);      % create an nbins-point Hann window

IPG=-pow2db((sum(w.^2)/nbins)); % incoherent processing gain for the
window

% reshape I/Q data into a 2D array; sqrt(2) adjusts for single sided
FFT
Ym=w.*reshape(Y/sqrt(2),nbins,int32(size(Y,1)/nbins));

% determine an adjustment factor (in dB) that factors in processing
gain,
% 50 Ohm input impedance and converts from dBW to dBm
Gadj=IPG-pow2db(50)+30;

% express it in linear units
gadj=10^(Gadj/10);

% calculate power per binbw (kHz) at the PXA input
pmW=(abs(fftshift((1/nbins)*fft(Ym,nbins)'))).^2)*gadj; % (in mW)
pdBm=pow2db(pmW); % and in dBm

% determine bin center frequencies and time increments
fcenter=FreqValidMin+(FreqValidMax-FreqValidMin)/2;
f=(1:nbins)* binbw -(nbins/2)* binbw +fcenter - binbw/2;
t=(((1:(length(Y)/nbins))-1))*XDelta*nbins;
```

4.2 System Calibration

Aggregate interference models use the victim receiver's antenna terminal as the reference plane. Likewise, to simplify the interpretation of the results (via a simple comparison of measurement test antenna gain to victim receiver antenna gain), we reference power measurements to the antenna terminal through a Y-factor calibration [8] which yields the net gain between the antenna

terminal and the input of the test instrument. Note that test equipment manufacturers handle this derivation in two steps. First, they determine the Y-factor for the measurement instrument itself. Then they determine the Y-factor due to the cascade of the device under test (DUT) and the instrument. Finally, the Y-factor of the instrument is backed out to determine the Y-factor of the DUT itself. In our situation, the PXA is an integral part of the measurement system, so the Y-factor of the PXA does not need to be determined for system calibration purposes—though its determination is essential for calculating the system G/T.

We use a calibrated noise diode that generates 20.9 dB of noise in excess of kTB at 1745 MHz. The excess noise raise is defined as the ratio of the difference between diode on and off temperatures to the standard temperature:

$$enr = \frac{T_{on} - T_{off}}{T_0} \text{ or in decibels, } ENR = 10log(enr) \text{ (dB)} \tag{34}$$

If we assume the noise diode temperature is 290K when off, then $T_{off} = T_0$ and

$$enr = \frac{T_{on} - T_0}{T_0} \tag{35}$$

So

$$T_{on} = (enr+1)T_0 \tag{36}$$

The y-factor (expressed in lower case to indicate linear units) is the ratio of the measured power at the PXA with the noise diode on and off:

$$y = \frac{n_{on|Ant}}{n_{off|Ant}} = \frac{T_{on}}{T_{off}} \tag{37}$$

First, the noise diode is connected to the end of the feed coax that mates with the antenna. The measured noise at the PXA with the noise diode on is due to the contribution of the noise diode and the internal noise of the system, referenced to the antenna terminal, which are then amplified by the net gain of the system, g_{sys}:

$$n_{on|Ant} = (kT_{on}B+kT_{sys}B)g_{sys} \tag{38}$$

Next, the noise diode is turned off and another measurement performed:

$$n_{off|Ant} = (kT_{off}B+kT_{sys}B)g_{sys} \tag{39}$$

so

$$y_{sys} = \frac{n_{on|Ant}}{n_{off|Ant}} = \frac{(kT_{on}B+kT_{sys}B)g_{sys}}{(kT_{off}B+kT_{sys}B)g_{sys}} = \frac{T_{on} + T_{sys}}{T_{off} + T_{sys}} \tag{40}$$

Solving for T_{sys} and recognizing that $T_{on} = (enr+1)T_0$ and $T_{off} = T_0$ yields:

$$T_{sys} = \frac{T_{on} - y_{sys}T_{off}}{y_{sys} - 1} = \frac{(enr+1)T_0 - y_{sys}T_0}{y_{sys} - 1} = \frac{(enr+1 - y_{sys})T_0}{y_{sys} - 1} \tag{41}$$

Substituting T_{sys} in the noise factor equation yields:

$$f_{sys} = 1 + \frac{T_{sys}}{T_0} = 1 + \frac{(enr+1 - y_{sys})T_0}{(y_{sys} - 1)T_0} = \frac{enr}{y_{sys} - 1} \tag{42}$$

Converting to noise figure, $F_{sys} = 10\log(f_{sys})$, and expressing the enr in decibels, $ENR = 10\log(enr)$:

$$F_{sys} = ENR - 10\log(y_{sys} - 1) \tag{43}$$

We also require the net gain of the system, g_{sys}, i.e. the gain between the antenna terminal and the input of the PXA. This is found by subtracting the internal noise generated by the system (when the noise diode is off) from each of the noise diode on measurements:

$$g_{sys} = \frac{n_{on|Ant} - n_{off|Ant}}{n_{on|PXA} - n_{off|PXA}} \tag{44}$$

In practice, the PXA gain and noise figure can be determined by performing 1 second long I/Q captures with the noise diode connected directly to the input of the PXA for both on and off conditions. The noise power (pmW from Section 4.1) for each capture is then averaged over 15,000 FFTs, i.e. pmW_PXAOn and pmW_PXAOff. The noise figure of the PXA as a function of frequency is then:

```
PXA_NoiseDiodeOn=mean(PmW_PXAOn,1);
PXA_NoiseDiodeOff=mean(PmW_PXAOff,1);
PXA_Yfactor=PXA_NoiseDiodeOn./PXA_NoiseDiodeOff;
ENR=20.92;  % dB
NF_PXA=ENR-pow2db(PXA_Yfactor-1);
```

The noise diode measurement is then repeated with the noise diode at the antenna reference plane, i.e. the end of the jumper that mates with the antenna. Computation of the net gain of the system from the antenna to Rx reference planes is then:

```
NoiseDiodeOn=mean(PmW_AntOn,1);
NoiseDiodeOff=mean(PmW_AntOff,1);
Gain=pow2db((NoiseDiodeOn-NoiseDiodeOff)./(PXA_NoiseDiodeOn-
PXA_NoiseDiodeOff));

Yfactor=NoiseDiodeOn./NoiseDiodeOff;
NF_sys=ENR-pow2db(Yfactor-1);
```

Figure 7 illustrates typical mean noise powers for a calibration cycle performed in a field measurement using a sampling rate of 15.36 MSa/s which is optimal for a 10 MHz LTE uplink band.
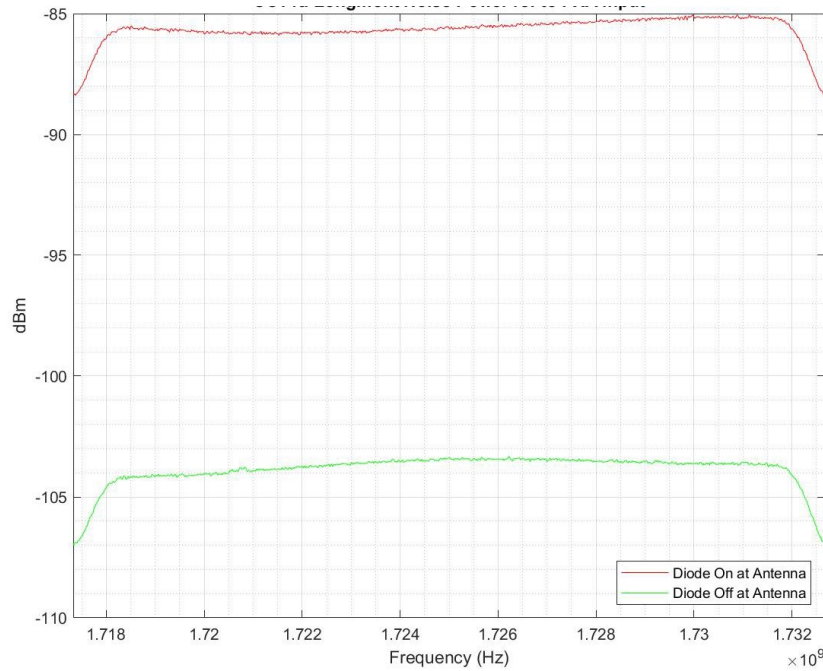
Figure 7. Noise power measurements over the total capture bandwidth.

Figure 8 shows the associated system gain and noise figure. Note that the noise power rolls off at both edges of the band. This is a characteristic of the PXA's internal anti-aliasing filter which engages outside the VSA's span. As previously mentioned, the span is related to the sampling rate, i.e. sampling rate = 1.28 × span. In this instance, with a span of 12 MHz there is no influence from the anti-aliasing filter on the measurement of the uplink band which has an occupied bandwidth of 9 MHz.
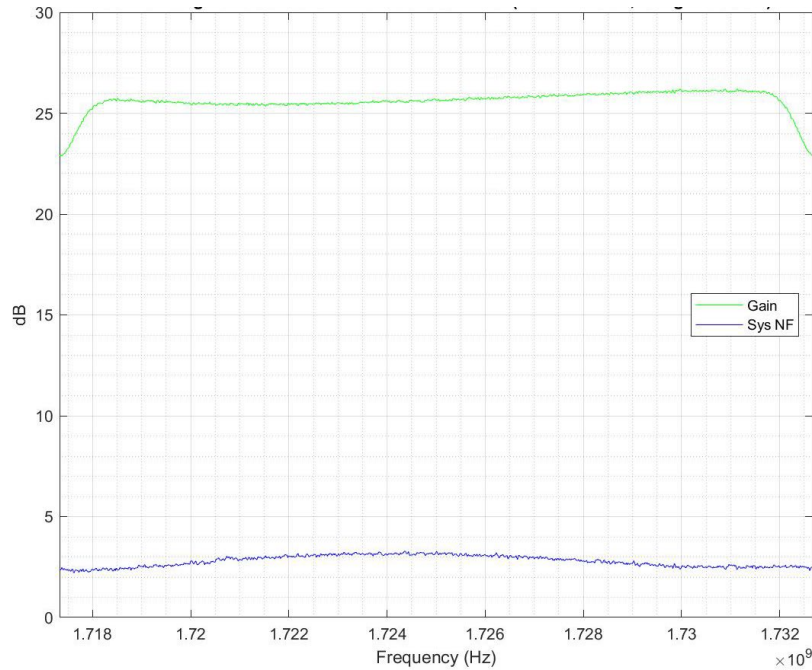
Figure 8. System gain and noise figure over the total capture bandwidth.

Once the net system gain has been determined, the measured power per FFT bin can be translated to the antenna reference plane:

```
pdBm_Ant=pow2db(pmW)-Gain; % in dBm
```

4.3 Statistical Analysis

Through a series of trial measurements and sponsor-led test planning and data analysis meetings a variety of techniques were developed to gain insights into LTE uplink occupancy and channel power in various bandwidths. A brief description of data collection approaches and standard post-processing products follows.

Data storage requirements are a key driver of the duration and frequency of I/Q captures. The typical LTE band of interest has a 10 MHz bandwidth, so according to Table 3 a sampling rate of 15.36 MSa/s is optimal. Since the VSA assigns 4 bytes each to I and Q values, the resulting I/Q capture uses 120 MB of memory for each second of capture. (Other bandwidths will scale linearly, i.e. a capture using a 20 MHz bandwidth will occupy 240 MB per capture second.) Over the course of several measurement events a capture duration of 10 s was found to yield a sufficient number of data points for development of the desired metrics (described below). The resultant captures occupy 1.2 GB each. Various capture intervals were investigated. The main driver in this case is providing sufficient time between captures for the instrument to transfer data and, if required, perform an internal system calibration. For 10 s long 1.2 GB captures, more than 3 minutes are required to perform these tasks, so a capture interval of 5 minutes was chosen for its simplicity. Consequently, a 24 hour long measurement campaign requires $1.2 \times 12 \times 24 = 345.6$ GB of memory. A three-day measurement event sufficient to demonstrate diurnal variations in captured power will thus require more than 1 TB of hard drive storage.

21

Waterfall plots are generated for each I/Q capture to provide a visual indication of channel occupancy and power as shown in Figure 9. To resolve control channel activity which occupies 0.5 ms timeslots, the plots are scaled to show 100 ms time intervals. In practice, only one or two snapshots are required for each capture to gain a qualitative sense of channel loading. Other data analysis products provide quantitative assessments of channel conditions over the entire capture duration.

The system under observation in this instance had three physical uplink control channels (PUCCHs) at the lower and upper edges of the band; the UE uses these channels to report channel quality, acknowledge messages, and make scheduling requests. The system also had 44 physical uplink shared channels (PUSCHs) in the center used to transmit user data. PUSCH transmissions in 1 ms timeslots are clearly distinguishable from PUCCH activity transmitted in 0.5 ms slots. Note the 1 and 3 PRB equivalent bandwidths annotated within the guard bands. These are used to assess the system noise floor in analyses to be discussed later.
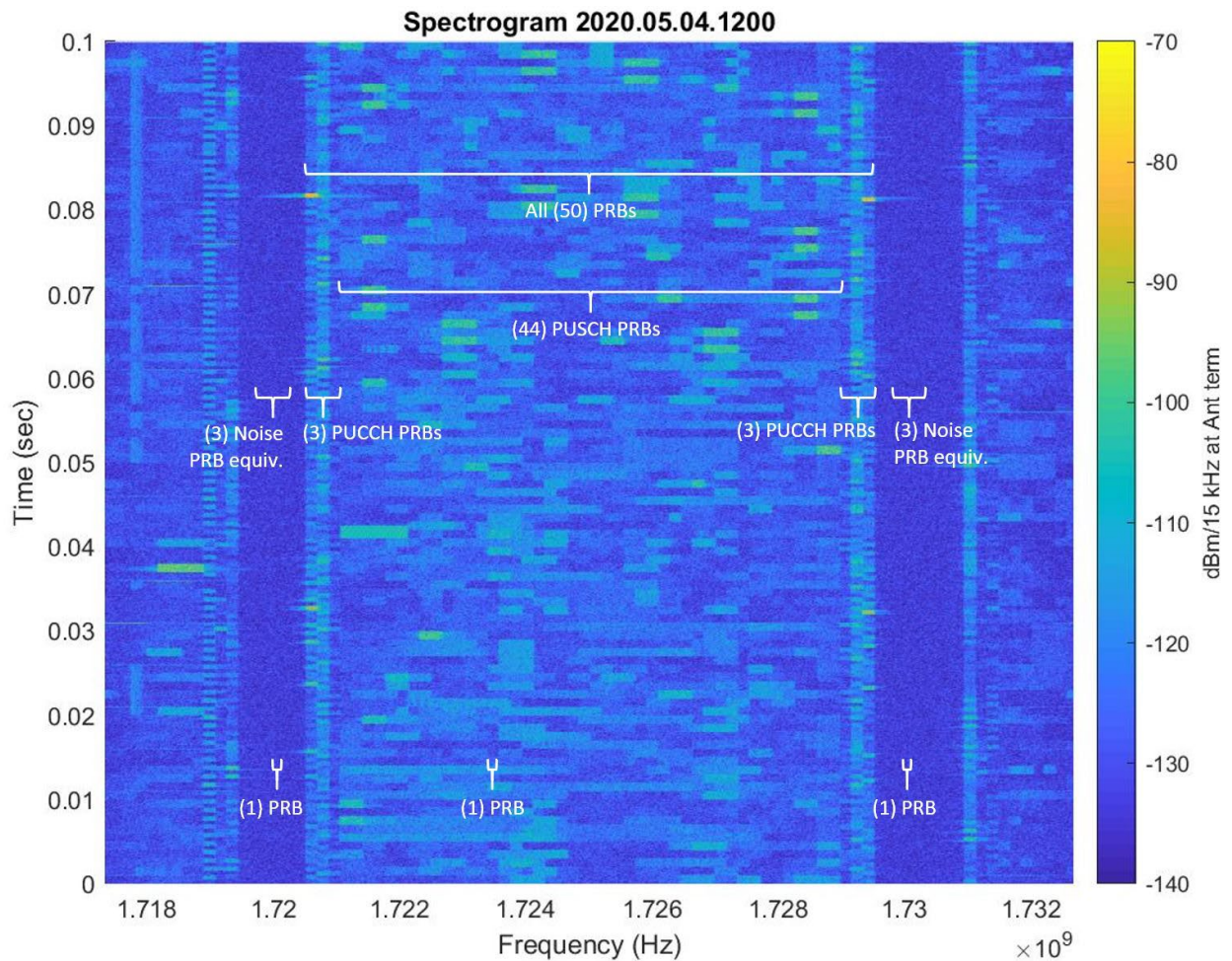
Figure 9. Spectrogram showing 100 ms of LTE UE uplink activity and channelization

Figure 10 shows an ensemble of cumulative distribution functions (CDFs) for a 10 MHz band which has 50 PRBs. Each trace is developed by summing power (in mW) across the (12) 15 kHz

22

FFT bins associated with each PRB. For a 10 second capture this yields 150,000 data points per PRB. The CDFs are produced using 0.1 dB increments in power. For reference, the two leftmost traces indicate the system noise floor in the lower and upper guard bands and are produced in a similar manner by summing across 12 FFT bins which are centered 450 kHz outside the edges of the occupied bandwidth as shown in Figure 9.
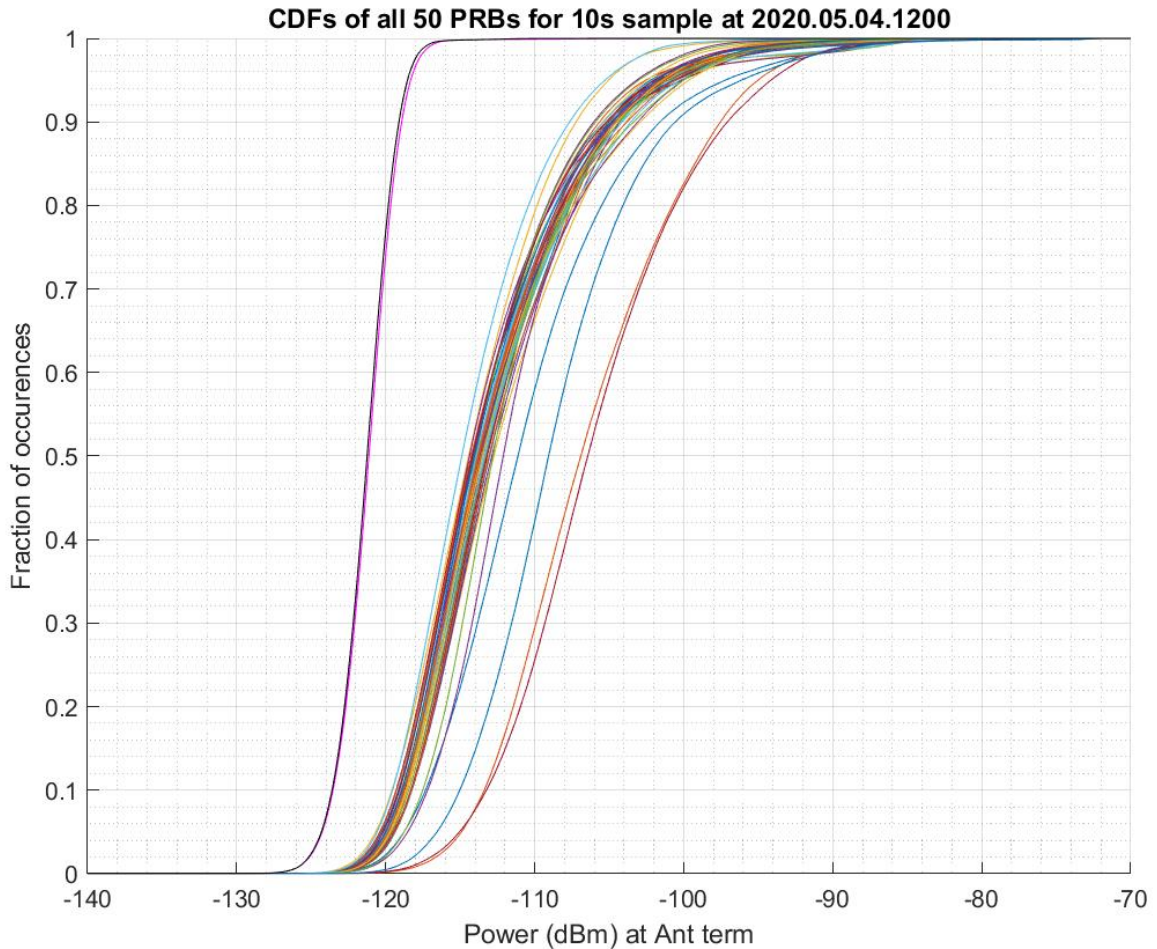
Figure 10. CDFs of PRB power for a 10 second capture

Several characteristics of this plot deserve further explanation. First, as will become evident later, the 4 rightmost traces correspond to the outermost PUCCHs (PRBs 0, 1, 48, and 49). These are typically stronger in power than the PUSCHs, since signaling from all UEs is aggregated in these few PRBs. Also, the impulsive nature of UE transmissions, which is indicated by elongated upper tails in a CDF, is evident at power levels exceeding -90 dBm. Finally, clustering of the CDFs is a useful indicator of how well the LTE scheduler uniformly distributes UEs within the band. In this instance, there is a large degree of uniformity as is shown later in Figure 12.

A number of other bandwidths are of interest to system modelers which permit direct comparisons to aggregate emissions model predictions. Some modeling tools simulate total

channel power across all PRBs in the band. ITS's Aggregate Emissions from LTE (AELTE) tool, on the other hand, only simulates traffic channel activity, so only power in the PUSCH PRBs is of interest. Power in the signaling channels, i.e. PUCCHs, at both edges of the band is found by computing CDFs for PRBs 0-2 and 47-49. Again, for reference to the system noise floor, guard band power is measured in a comparable 3 × 180 kHz bandwidth. The plot of CDFs for these special bandwidths is shown in Figure 11.
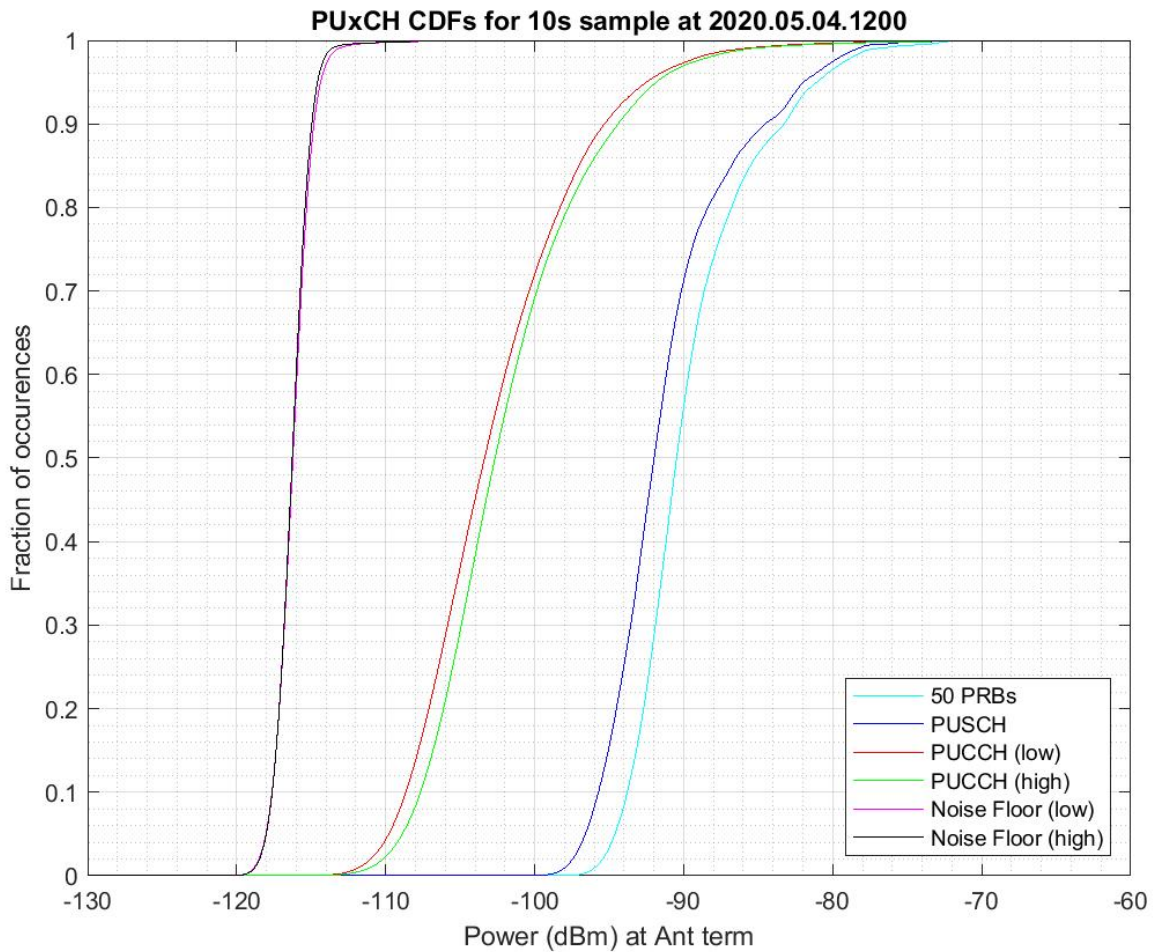
Figure 11. CDFs for special bandwidths

For better insight into the frequency dependence of power across a band, a spectrum contour plot (Figure 12) is of value. This is generated by computing CDFs of power in each FFT bin and plotting their contours at decile values from 100% to 10%. The uppermost trace, then, represents the maximum power in each 15 kHz bin for the duration of the capture—10 s in this instance—and is similar to the max hold function on a spectrum analyzer. Likewise, the next lower trace is the 90th percentile power. Control and traffic channels are labeled for reference. Note the elevated power in the PUCCH PRBs at both ends of the band (PRBs 0, 1, 48, and 49) which are particularly distinguishable at percentile values of 90 % and lower. The two remaining PUCCHs

(PRBs 2 and 47) carry less frequent scheduling requests, so their aggregate power is several dB lower on average than the other PUCCH or PUSCH PRBs.
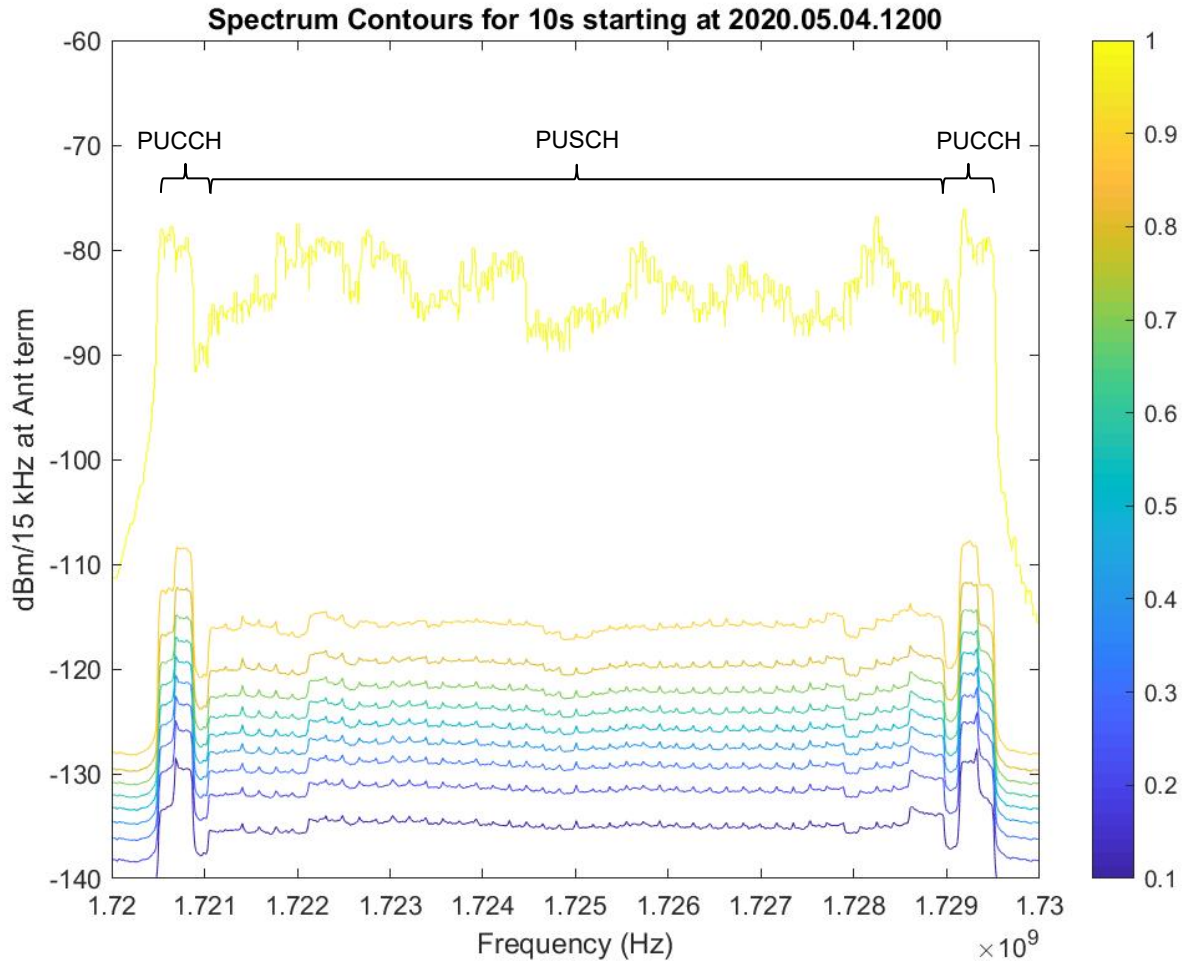
Figure 12. Spectrum contour plot

While a spectrum contour plot presents the data as a cumulative distribution of power in each FFT bin, a persistence plot (Figure 13) presents the probability density of power in each FFT bin. To generate this visualization power levels are broken down into 0.1 dB increments and a histogram of power for each FFT bin is created. After normalization by the count of FFTs in the capture, an ensemble of probability density functions is created. Each pixel in the image, which spans 0.1 dB in power and 15 kHz in frequency, is then color coded according to its frequency of occurrence. Note that many samples occur below the Y-axis lower limit of -140 dBm. These values are present in the PDF computation but are omitted in the graphic presentation to yield a more useful range of values.
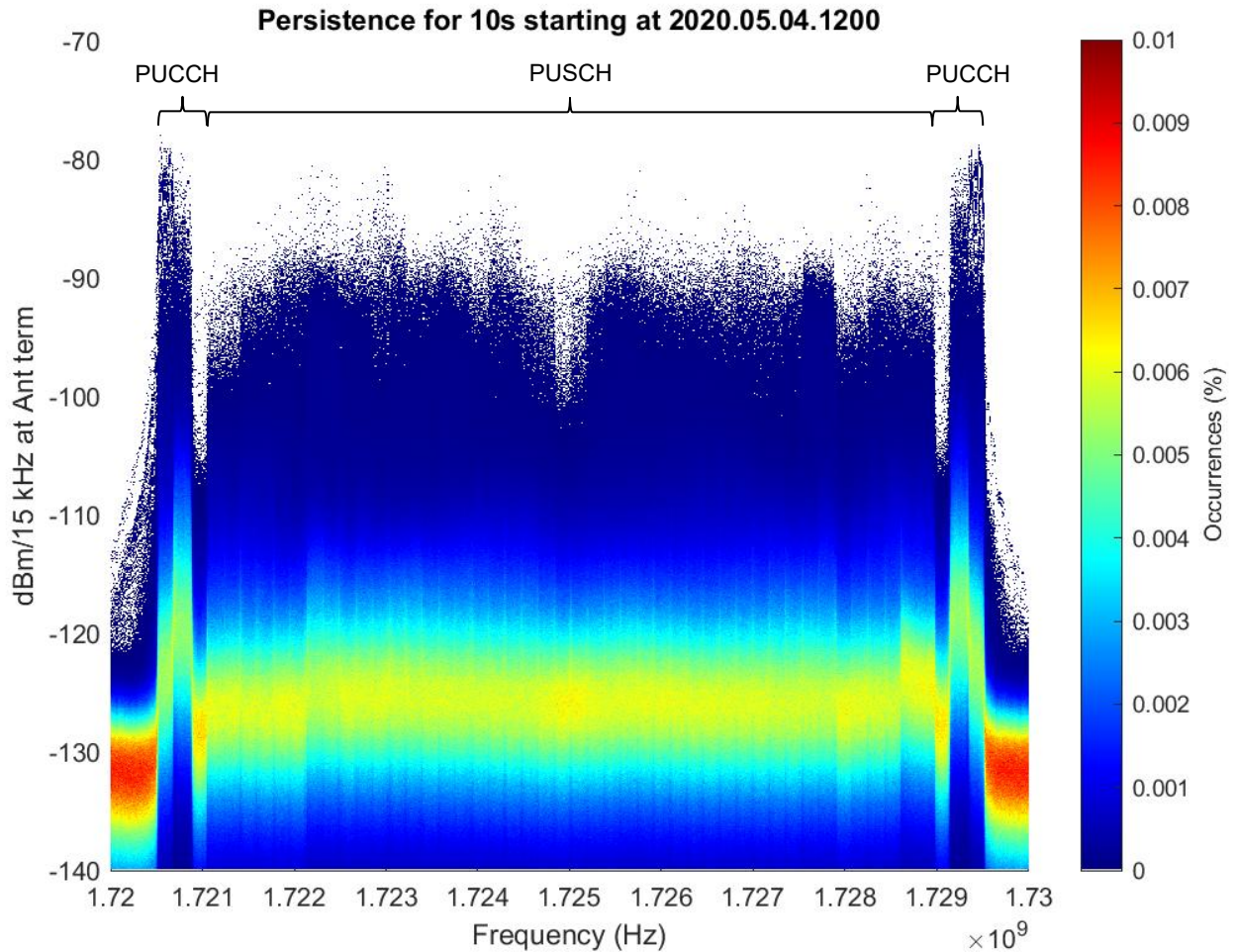
Figure 13. Spectrum persistence plot

Of particular interest to aggregate interference modelers is the variation of channel power throughout the day, since peak usage represents a worst case scenario from an electromagnetic compatibility or interference modeling standpoint. To facilitate such analyses, ITS developed instrument control scripts that can run unattended and trigger VSA captures at integer multiples of minutes. The only limitation to the duration of a measurement event is data storage. The system uses a pulse per second source from a GPS receiver to trigger at the top of the minute. As discussed earlier, this capture interval is typically set to 5 minutes. Figure 14 shows the variation in total channel power, i.e. 50 PRBs in this instance, from a measurement campaign which occurred over a 2+ day timespan with captures every 5 minutes. Each trace represents the CDF of channel power during each 10 second capture. The CDF percentile is color coded per the legend. The diurnal variation in power is immediately evident.
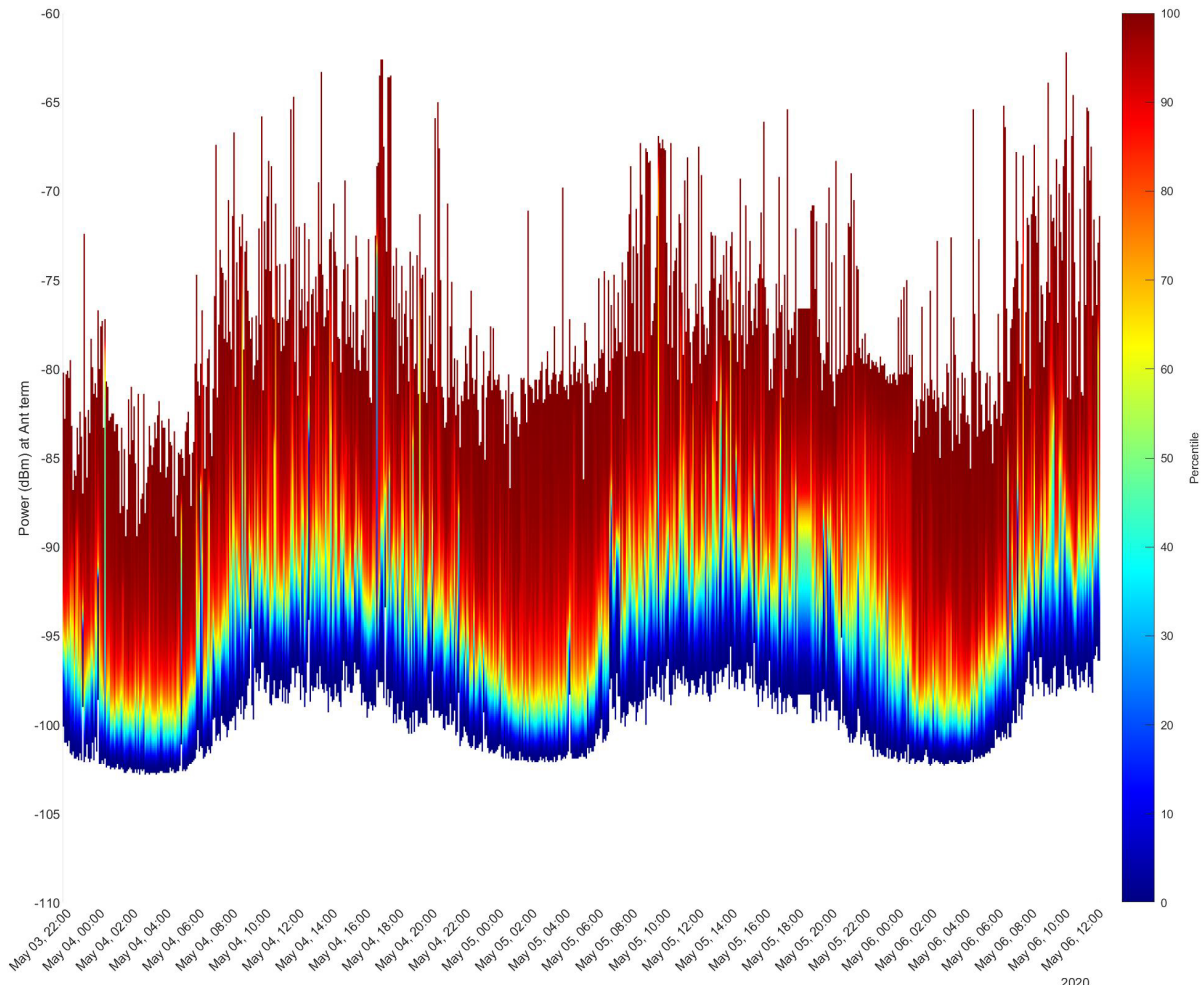
Figure 14. Time series plots of color-mapped channel power CDFs

Observe how the range of powers is compressed at night, for example from 2200 hours on 3 May to 0600 hours on 4 May, which then gives way to daytime busy hours ranging from approximately 0800 to 1800 hours with much greater peaks in relation to median (50th percentile) values. The pattern then repeats with a noticeable degree of diurnal regularity.

Since aggregate interference modelers are most interested in worst case conditions, they may, by visual inspection, select a range of daytime hours when aggregate power is greatest to guide the selection of measured power for comparison to model predictions.

5. CONCLUSIONS

ITS's LTE uplink aggregate measurement system has been fully automated to perform unattended I/Q captures over multiple days with hard drive storage limitations being the only practical limitation on measurement event length. Likewise, a suite of MATLAB based post-processing scripts can ingest the aforementioned net system gain curve so that power levels can be referenced to the antenna terminal, statistics generated for each capture, and summaries like that in Figure 14 created.

These data have been instrumental in gathering ground truth measurements at multiple times of the year and in multiple locations for use in model validation.

6. REFERENCES

[1]   Amendment of the Commission's Rules with Regard to Commercial Operations in the 1695-1710 MHz, 1755-1780 MHz, and 2155-2180 MHz Bands, GN Docket No. 13-185, Report and Order, 29 FCC Rcd 4610 (2014) available https://www.fcc.gov/document/fcc-sets-stage-auction-65-mhz-spectrum-mobile-broadband-0

[2]   Rec. ITU-R P.372-7 1 Radio noise available at https://www.itu.int/dms_pubrec/itu-r/rec/p/R-REC-P.372-7-200102-S!!PDF-E.pdf

[3]   H.T. Friis, *Noise Figures of Radio Receivers*, Proceedings of the IRE (Volume: 32, Issue: 7, July 1944)

[4]   T.Y. Otoshi, Calculation of Antenna System Noise Temperatures at Different Ports— Revisited, IPN Progress Report 42-150 August 15, 2002.

[5]   Keysight N9030B PXA User Manual available at http://rfmw.em.keysight.com/wireless/helpfiles/89600B/WebHelp/89600.htm

[6]   Telesystem Innovations Inc., *LTE in a Nutshell: The Physical Layer White Paper* accessed at https://home.zhaw.ch/kunr/NTM1/literatur/LTE in a Nutshell - Physical Layer.pdf 5/19/2020

[7]   Otis M. Solomon, Jr, *PSD Computations Using Welch's Method*, Sandia Report SAND91-1533, December 1991 available at https://www.osti.gov/servlets/purl/5688766/

[8]   *The Y Factor Technique for Noise Figure Measurements Application Note* available at https://www.rohde-schwarz.com/us/applications/the-y-factor-technique-for-noise-figure-measurements-application-note_56280-15484.html

[9]   Sklar, Bernard. *Digital communications: fundamentals and applications*. Englewood Cliffs, N.J: Prentice-Hall, 1988. Print.

ACKNOWLEDGEMENTS

BIBLIOGRAPHIC DATA SHEET

1. PUBLICATION NO. TM-21-552	2. Government Accession No.	3. Recipient's Accession No.

4. TITLE AND SUBTITLE LTE Uplink Aggregate Interference Measurement System	5. Publication Date February 2021
	6. Performing Organization Code NTIA/ITS.M

7. AUTHOR(S) Eric D. Nelson	9. Project/Task/Work Unit No. 6916000-300
8. PERFORMING ORGANIZATION NAME AND ADDRESS Institute for Telecommunication Sciences National Telecommunications & Information Administration U.S. Department of Commerce 325 Broadway Boulder, CO 80305	
	10. Contract/Grant Number.

11. Sponsoring Organization Name and Address Defense Information Systems Agency (DISA) Defense Spectrum Organization (DSO) 2002 Turbot Landing Annapolis, MD 21402-5064	12. Type of Report and Period Covered

14. SUPPLEMENTARY NOTES

15. ABSTRACT (A 200-word or less factual summary of most significant information. If document includes a significant bibliography or literature survey, mention it here.)

This technical memorandum describes a method to design, characterize and optimize a system for performing field measurements of aggregate interference from LTE user equipment transmissions. It explains the computation of the system's antenna gain over effective system temperature (G/T) and anticipated signal-to-noise ratio levels using typical assumptions. It also covers the appropriate vector signal analyzer settings for performing I/Q captures of LTE signals and relevant post-processing techniques.

16. Key Words (Alphabetical order, separated by semicolons)

uplink, LTE, UE, aggregate interference, I/Q, capture, G/T, noise temperature

17. AVAILABILITY STATEMENT ☒ UNLIMITED. ☐ FOR OFFICIAL DISTRIBUTION.	18. Security Class. (This report) Unclassified	20. Number of pages 43
	19. Security Class. (This page) Unclassified	21. Price:

NTIA FORMAL PUBLICATION SERIES

NTIA MONOGRAPH (MG)
A scholarly, professionally oriented publication dealing with state-of-the-art research or an authoritative treatment of a broad area. Expected to have long-lasting value.

NTIA SPECIAL PUBLICATION (SP)
Conference proceedings, bibliographies, selected speeches, course and instructional materials, directories, and major studies mandated by Congress.

NTIA REPORT (TR)
Important contributions to existing knowledge of less breadth than a monograph, such as results of completed projects and major activities.

JOINT NTIA/OTHER-AGENCY REPORT (JR)
This report receives both local NTIA and other agency review. Both agencies' logos and report series numbering appear on the cover.

NTIA SOFTWARE & DATA PRODUCTS (SD)
Software such as programs, test data, and sound/video files. This series can be used to transfer technology to U.S. industry.

NTIA HANDBOOK (HB)
Information pertaining to technical procedures, reference and data guides, and formal user's manuals that are expected to be pertinent for a long time.

NTIA TECHNICAL MEMORANDUM (TM)
Technical information typically of less breadth than an NTIA Report. The series includes data, preliminary project results, and information for a specific, limited audience.

For information about NTIA publications, contact the NTIA/ITS Technical Publications Office at 325 Broadway, Boulder, CO, 80305 Tel. (303) 497-3572 or e-mail ITSinfo@ntia.gov.